Multi-Band 3D Printed Frequency Selective Surface for RF Shielding Applications

Deepika Singh[1, *], Rana P. Yadav[2], and Hemdutt Joshi[1]

[1] *Thapar Institute of Engineering and Technology, Patiala, India*
[2] *Institute of Plasma Research, Gandhinagar, India*

ABSTRACT: This paper presents the design and development of 3D printed multi-band frequency selective surface (FSS) for RF shielding applications. The developed FSS significantly rejects the frequency at Wi-Fi, WiMax, and ISM/WiMax bands. The FSS has been fabricated using a 3D printed ABS substrate and metalized with a copper paint as per design. Its unit cell consists of three independent sub-geometries in which two are mostly like a concentric square loop that encircles the third one, i.e., modified Jerusalem structure. All of these sub-geometries are individually designed for the different rejection bands where their combination is optimized as a unit cell of FSS. The designed unit cell rejects the Wi-Fi, WiMax, and ISM/WiMax bands centered at 2.45 GHz, 3.5 GHz, and 5.8 GHz with attenuation level more than 35 dB. The developed FSS is a prototype of RF shielding structure to be utilized for the fabrication of an interference-free test chamber which isolates the Wi-Fi, WiMax, and ISM/WiMax interference. The design of FSS is very simple and can be printed in large scale for the development of shielding applications.

1. INTRODUCTION

Frequency selective surface (FSS) has a wide application scope which ranges from communication to defence. FSS presents a periodic arrangement of identical structures called unit cells [1] which can be utilized as pass/stopband filter. FSSs are applied in various fields for EMI (electromagnetic interference) reduction [2], filtering [3], RCS (radar cross section) reduction [4], antenna radomes [5], etc.

Because of its important applications, it is a current research interest. Researchers are working on EMI shielding in order to suppress the signals for security reasons and to avoid cross-coupling between the different wireless channels that are in close proximity with each other. It has been found that WLAN/Wi-Fi and WiMax signals are mainly used in communication, and these significantly introduce interference to other important wireless networks. The isolation of important areas like defence sites, medical facilities (ICU), prison cells, worship places, etc. from unwanted radio signals [6] has become a key concern nowadays. Hence, printing based FSS turns out to be the best alternative to stop the transmission of WLAN and WiMax signals.

Various earlier investigations have been found in this reference in current literature. A compact dual-band FSS has been presented earlier for WLAN applications [7]. Additionally, a polarization independent bandpass FSS has been developed for WiMax applications [8]. It consists of a customized plus-shaped structure within a ring-shaped and a square ring. A triple band FSS is proposed for WLAN, WiMax, and X-band applications [9]. However, this is a double sided structure which introduces complexity in mass production. Apart from it, all other

structures also possess some merits, but there are certain issues which need to be solved, like complex structure that makes fabrication difficult and multi-layered structure that increases fabrication cost, size, and even time. Even all these geometries are mostly fabricated using PCB (printed circuit board) technique that is costly and often requires complicated procedures. Hence, it is required to adopt a cost effective technique that can overcome all these shortcomings of traditional PCB technique. 3D (three-dimensional) printing came into effect and can be used for fabrication of any planar or non-planar geometry [10]. This printing technique has an advantage in terms of manufacturing time and fabrication cost. Hence, this technique can be used for rapid prototyping.

In this paper, a multi-band FSS has been designed and developed for the application of radio frequency (RF) shielding. The designed FSS has been fabricated using 3D printed ABS substrate and metallized using copper paint. The FSS has been developed for the rejection of Wi-Fi, WiMax, and ISM/WiMax applications with attenuation level more than 35 dB. The proposed FSS geometry consists of a modified Jerusalem cross structure within two square loops. Using 3D printing material, complex structures can be easily fabricated and in a cost effective manner. In this way, fabrication cost of FSS is rapidly reduced in order to meet the demand of future applications. This paper is mainly based on the fabrication of a frequency selective surface using 3D printing technique, where we have investigated the performance of FSS for various fabrication tolerances and also reliability in terms of cost effectiveness for production in contrast to the available techniques. However, 3D printing introduces fabrication tolerance because of limited precision which can deteriorate the performance of FSS. Study outcomes have been demonstrated using the fabrication and test-

---

* Corresponding author: Deepika Singh (deepikasingh806@gmail.com).

ing of FSS. The unit cell of FSS is designed in such way that it can be easily printed and also easy to metalize. These cells are also robust to absorb the printing tolerances, and their effect is compensated mutually, as found in results. The challenges related to the fabrication of FSS using 3D printing have been comprehensively addressed in this paper. The presented work is important for the rapid prototyping of FSS like RF structure and its large scale for production which is mainly required for RF shielding and filtering.

2. FSS UNIT CELL DESIGN AND ANALYSIS

The unit cell of the proposed FSS consists of a modified Jerusalem cross within a modified square loop and enclosed inside another square loop. It is printed on the single side of the substrate. A few basic steps have been followed while designing the FSS. The design process of any FSS starts with unit cell design. The proposed unit cell consists of modified Jerusalem cross inside two square loops out of which slots are cut in inner square loop. The square loop is well studied in literature. The equivalent circuit model (ECM) analysis of square loop is used for extracting the values of L (Inductance) and C (Capacitance) by [11] using physical parameters of FSS. The basic equations for the calculation of L and C is explained by [11] where inductive reactance and capacitive susceptance are described as:

$$\frac{X(w)}{Z_0} = F(p, w, \lambda) \tag{1}$$

$$\frac{B(g)}{Z_0} = 4F(p, g, \lambda) \tag{2}$$

where $F(p, w, \lambda) = \frac{p}{\lambda} \cos \theta [\ln(\operatorname{cosec} \frac{\pi w}{2p}) + G(p, w, \lambda)]$, G is the correction term; p is the periodicity; w is the width of conducting loop; and g is the gap between conducting loops.

Firstly, it is required to find the loop size at desired resonant frequencies for designed structure. The approximate analysis of finding loop parameters like loop size of single square loop FSS is explained by [12].

$$1 = 4 \left(\frac{p_1}{\lambda}\right)^2 x \ln \left[\frac{2p}{\pi w_1}\right] \tag{3}$$

In order to avoid grating lobes

$$p(1 + \sin \theta) < \lambda \tag{4}$$

Consider that the inequality of above equation is satisfied, taking $p = M\lambda$, where M is the constant having value between 0 to 1. So, substituting above equation in (3), the equation can be rewritten as:

$$1 = 4 \left(\frac{p_1}{\lambda}\right)^2 x \ln \left[\frac{2M\lambda}{\pi w_1}\right] \tag{5}$$

Using above equation with w_1/λ ratio as 0.005, the approximate outer loop length p_1 is obtained as 28.3 mm. With w_2/λ ratio as 0.03, middle loop length (l) is approximately obtained as 25.2 mm. There are some parametric and other assumptions taken, and these calculated values are approximate values. The

loop lengths are optimized for desired frequencies. The periodicity must satisfy Equation (4) in order to avoid grating lobes. The slots cutting at the middle of second square loop results in meandering in path that helps in lowering frequency to desired frequency band. The Jerusalem cross structure is also modified to increase path length of structure in order to reduce upper resonant frequency.

Initially, loops have been designed and simulated on an individual basis to get better analysis about the pass and stopbands using simulation results; then its combination has been optimized to get the final design of the unit cell. The layout of the unit cell is presented with different dimension parameters shown in Figure 1 whose values are given as $p = 23.5$ mm, $l = 20$ mm, $l_1 = 12.8$ mm, $l_2 = 7$ mm, $w_1 = 0.65$ mm, $w_2 = 2.75$ mm, $w_3 = 1$ mm, $a_2 = 1.5$ mm, $b_1 = 2.5$ mm. The overall thickness of the substrate is 1.5 mm, which is grooved inside with 0.5 mm deep at a place where it is to be metalized. The unit cell is metalized with copper paint. It is fabricated with ABS using 3D printing where metallic and non-metallic portions inside the unit cell are represented by yellow and white colours, respectively. The ABS used in fabrication has a dielectric constant of 2.8. Figure 2(d) shows the final version of the unit cell resonating at 2.45 GHz, 3.5 GHz, and 5.8 GHz for stopbands. It provides 41 dB, 35 dB, and 46 dB attenuation at the center frequencies under the stopbands with a corresponding 10 dB bandwidth of 0.46 GHz, 0.26 GHz, and 1.68 GHz, respectively. FSS is designed to reflect in some selective frequencies which are mainly decided by FSS design parameters. The surface current distribution obtained from the simulation at different center frequencies is shown in Figure 3. The corresponding loops have a maximum current density at their resonant frequency, for example at 2.45 GHz, and the outer loop has a maximum current density. As usual, when frequency increases, the current density pattern is mostly shifted from outer to center and found maximum in center at modified Jerusalem cross at 5.8 GHz. The current is mostly confined at the edges of the metallic strip. In addition, incorporated stepping in the middle loop reduces the linear current density at edges of loop strip which compensates the unit cell to get the resonance frequency lower than usual.
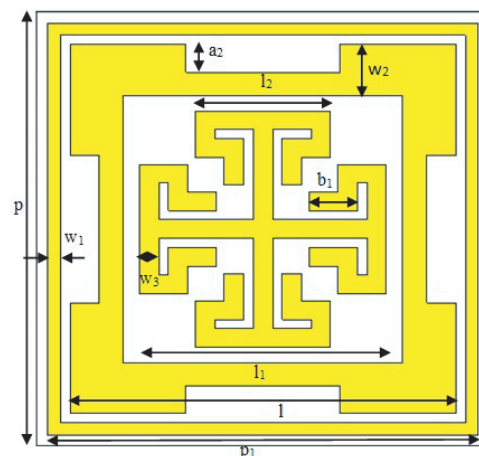
FIGURE 1. Proposed Unit cell structure.
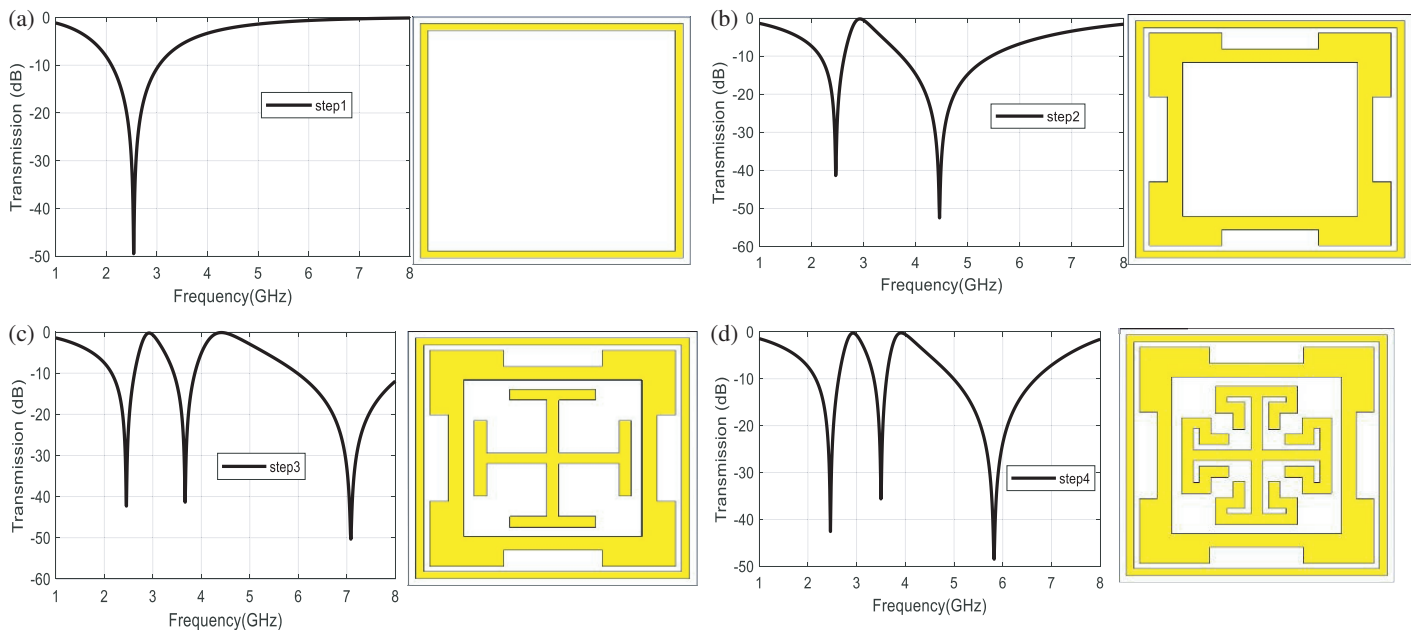
FIGURE 2. Steps of Unit Cell (a) Step 1, (b) Step 2, (c) Step 3, (d) Step 4.
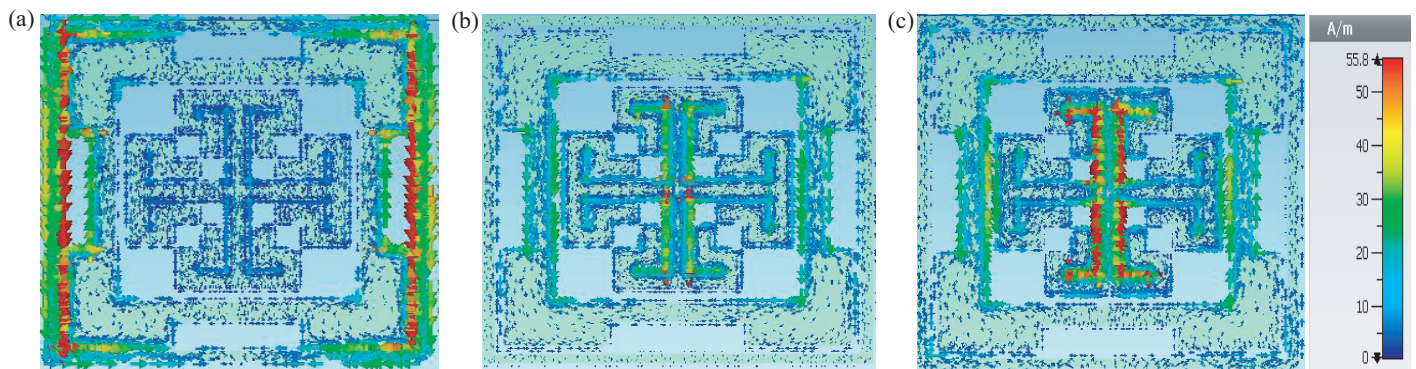
FIGURE 3. Surface current distribution (a) 2.45 GHz, (b) 3.5 GHz, (c) 5.8 GHz.

3. PERFORMANCE ANALYSIS

3.1. Parametric Analysis

Performance of FSS can be optimized by changing the unit cell parameters. Their effects have been comprehensively analyzed and presented as follows:

- In the outermost conducting loop, the change of dimension of w_1 in outward direction in the range of 0.35–0.95 mm significantly changes the lower stopband and shifts the center frequency in the range 2.57 GHz–2.35 GHz, whereas its effect on other stopbands is very insignificant as compared with lower stopband as seen in Figure 4(a).

- The change in the dimension of stepping in the middle conducting loop mostly affects the upper and middle stopbands where its effect on the middle one is less significant whereas slight change has been noticed at the lower stopband as shown in Figure 4(b).

- The modification in different segments in modified Jerusalem cross mostly affects the upper and middle

bands whereas the stopband centered at 2.45 GHz remains unchanged. Figures 4(c) and (d) can be referred for more details where the effects of change in l_1 and l_2 have been presented.

3.2. Stability Analysis

This section examines the effect of variation in different incident angles and polarizations. An incident wave can hit the FSS structure from any angle, so it must remain stable under different incident angles and different changing environmental conditions. Figure 5 shows the incident angle performance for TE and TM modes. FSS exhibits better stability for middle stopband while a large variation is observed in upper stopband frequency above 20°. The frequency deviation for upper stopband up to 20° incident angle has been found approximately 4% and 1% for TE and TM modes, respectively which can be usually expected [13]. It became more significant after 20°, mainly for TE mode and found approximately 11.55% at 50°
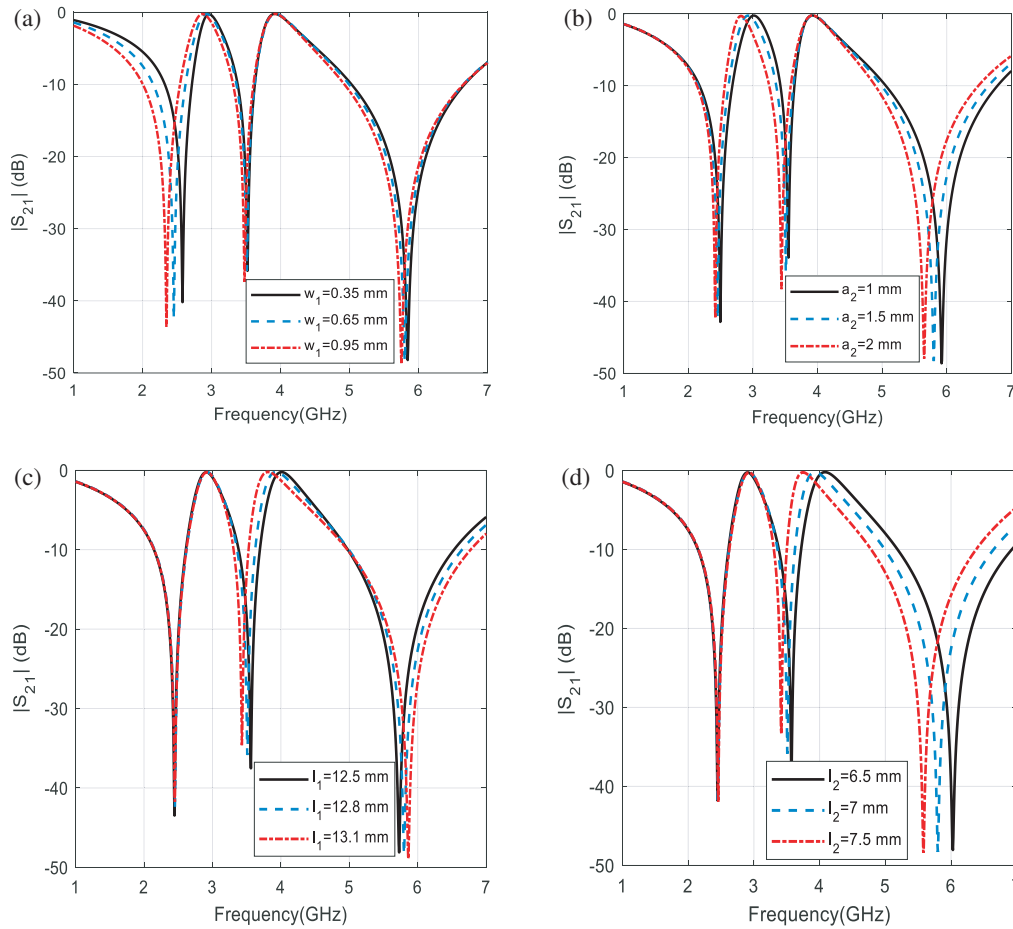
FIGURE 4. Parametric analysis of proposed structure. Effect of (a) w_1, (b) a_2, (c) l_1, (d) l_2 on structure.

angle. TE mode is more sensitive in angular term because of discontinuity arises due to the angular projection of grooving and metallization. In lower resonating band, frequency deviation is less than 4% for both the modes up to incident angle $50°$ which is under desired limit. A little more deviation can also be contributed because of grooving the substrate instead of using planar substrate because 3D printed structure is more like planar with track slots plated with copper paint. This slot came with the vertical projecting and produces electrical discontinuity. Its resultant effect can be observed as a shift in frequency band as seen in Figure 5. It can be observed that frequency shift mainly at upper band becomes more significant when grooving is incorporated. As seen in Figure 5(c), by reducing grooving height, resonating bands are closer than groove. But it also affects the desired resonating bands.

4. EQUIVALENT CIRCUIT MODEL (ECM) ANALYSIS

The equivalence FSS unit cell is analysed using a lumped equivalent circuit model in general. The ECM of the designed FSS unit cell is shown in Figure 6(a) which is presented with a parallel combination of three segments, including the capacitor and inductor connected in series. Each of the loops can present the single inductance and capacitance values which are connected in series. When a plane wave imposes on the surface of FSS,

electric charge density is created in adjacent strips, which produces capacitance while magnetic field created in the loop due to the flow of electric current produces inductance. Inductance is created from loop areas while capacitance is obtained from gaps between adjacent elements [14]. The unit cell of FSS consists of three individual loops which are presented with the individual inductances and capacitances L_1, C_1, L_2, C_2, L_3, and C_3 from outer to inner loop. This parallel combination equivalence is represented with L_m and C_m in Figure 6(a).

The surface impedance of loops based on the lumped parameters is given as,

$$Z_m = j\omega L_m + \frac{1}{j\omega C_m} = \frac{1 - \omega^2 L_m C_m}{j\omega C_m} \qquad (6)$$

where $j\omega L_m$ and $\frac{1}{j\omega C_m}$ are reactance related with L_m and C_m, respectively.

The circuit model is simulated using ADS software, and results are found in good agreement with electromagnetic simulation as shown in Figure 6(b).

5. FABRICATION SETUP AND EXPERIMENTAL RESULTS

The designed FSS has been fabricated using 3D printing where ABS is used as a dielectric. For metallization, a copper paint is
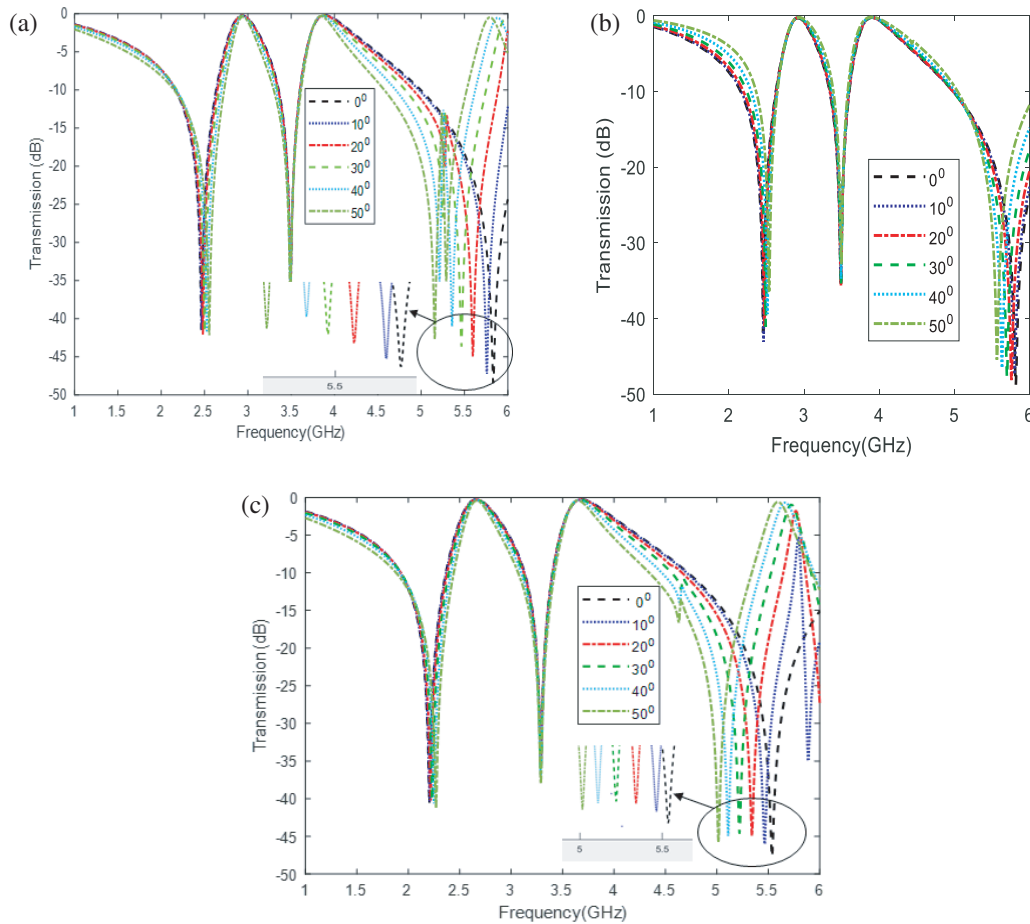
FIGURE 5. Transmission parameter of different angles for (a) TE mode, (b) TM mode, (c) TE mode with reduced groove height.
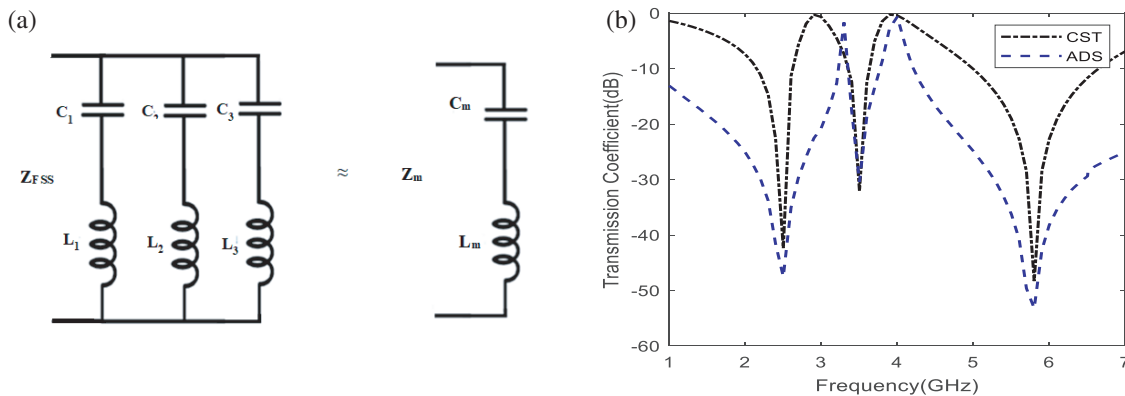
FIGURE 6. (a) Circuit model of design FSS, (b) comparison of electromagnetic simulation and ADS simulation of proposed FSS.

used having surface conductivity of 0.3–0.7 ohms per sq., attenuation of 75 dB at coating thickness of 50 micron. The coating for metallization on the surface of elevated part is done manually using paint brush with conductive paint (silver coated copper screening compound) where coating is applied repeatedly two to three times so that conductivity is achieved. The fabricated FSS consists of an array of 8×6 unit cells where the size of a single unit cell is 23.5 mm $\times$ 23.5 mm, and the complete structure is 188 mm $\times$ 141 mm in total as shown in Figure 7.

The overall thickness of the structure is 1.5 mm which is grooved with a height of 0.5 mm. By grooving the substrate, it becomes easy to apply conductive paint where the surface is to be metallized. The fabricated structure is slightly rough. The surface smoothness of structure basically depends on quality of 3D printing. 3D printing is not a precise method for printing high sensitive structures. Surface roughness mainly produces losses at very high frequency. It has considerable effect in resonating frequency bands. Only elevated part of the surface is
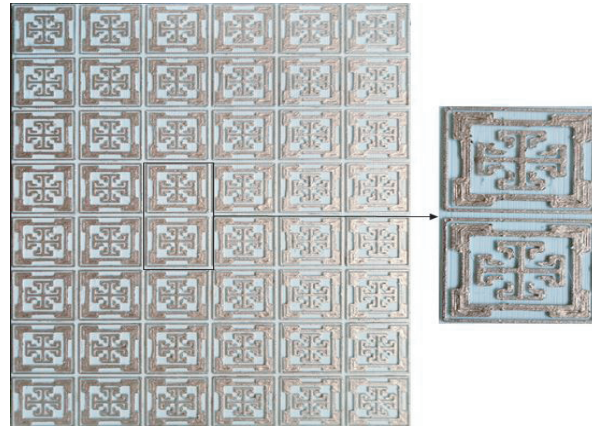
FIGURE 7. Fabricated prototype.
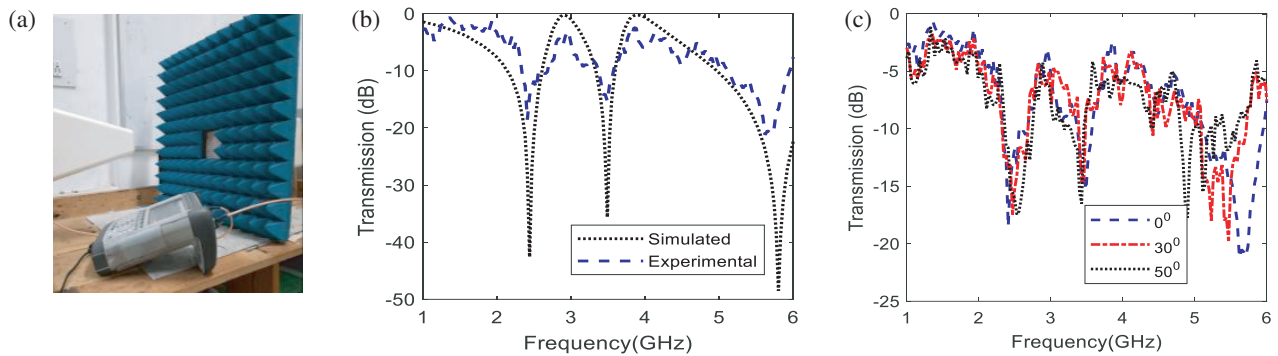
FIGURE 8. (a) Experimental setup, (b) comparison of simulated and experimental result, (c) experimental result of TE polarization.

TABLE 1. Comparison table of present work with earlier designed structures.

Ref	Unit cell size	Operation frequency (Single/Double/Triple band)	Fabrication Technique	Angular stability
[15]	$0.144\lambda_0 \times 0.144\lambda_0$	Triple band 942 MHz, 1842 MHz and 2142 MHz	PCB	$45°$
[16]	$0.117\lambda_0 \times 0.117\lambda_0$	Single band 5 GHz	PCB	$60°$
[17]	$0.142\lambda_0 \times 0.142\lambda_0$	Dual band 930 MHz and 1720 MHz	Paper substrate	$60°$
[18]	$0.248\lambda_0 \times 0.248\lambda_0$	Dual band 8.47 GHz and 10.45 GHz	PCB	$60°$
Proposed structure	$0.191\lambda_0 \times 0.191\lambda_0$	Triple-band 2.45 GHz, 3.5 GHz and 5.8 GHz	3D printing	$20°$

metallized using copper paint, so it rarely spreads over the undesired region. It can be removed in case found at a few places. Here, our main motive is to develop a reliable and cost-effective method for the fabrication of FSS.

For the measurement of transmission parameter S_{21}, FSS is placed between two antennas which are connected with VNA ports. The measurement is done using the combination of log-periodic and Vivaldi antennas due to unavailability of wideband horn antenna. A photograph of the experimental setup is shown in Figure 8(a). First, the measurement is done without keeping the FSS in between in order to validate path loss. Then, FSS is kept in between to measure the transmission parameter. It can be seen that measured results are in good agreement with simulated ones as given in Figure 8(b). The measured re-

sults verified all three rejection bands with center frequencies at 2.42 GHz, 2.49 GHz, and 5.71 GHz as compared with simulation results of 2.45 GHz, 3.5 GHz, and 5.8 GHz for lower, middle, and upper rejection bands, respectively. It provides a little deviation of less than 2% for lower and upper frequency bands and less than 1% for middle band at center frequencies for normal incidence. Overall band rejection is found better than -15 dB. The result variations in measured results are influenced by manufacturing errors that occur during fabrication, due to finite length of fabricated structure, and losses during measurements. The passband losses may be due to conductive losses and surface roughness that cause scattering and reflection. Substrate fabrication using 3D printing is not up to the mark in reference to surface roughness and uniform density of

material. 3D printing is still evolving, and material properties are still challenging to find which can vary for materials taken in simulation, so this kind of tolerance can be expected in measurement. The measurement results of TE polarization are also presented in Figure 8(c). The performance of measured results are deteriorating as angle increases mainly for upper rejection band. Test results show that the fabricated FSS provides the desired outcome which can be useful for many important applications like Wi-Fi, WiMax, etc.

To analyse the significance of the work done in the manuscript a comparative study has been presented in Table 1. It compares the work presented in the manuscript with the earlier investigations in aspects of performance and fabrication techniques mainly by taking into the consideration of shielding applications. As seen from Table 1, the designed FSS structure has more resonating bands than the work presented in [16–18]. Presented work has cost effective fabrication technique as compared with others, and it helps in rapid prototyping. This method is not good in consideration of angular stability.

6. CONCLUSION

In this paper, the design and development of a multi-band FSS is presented. It is fabricated using a 3D printing technique and metalized using copper paint as per the design. The FSS design is simulated using CST microwave studio software. Size of the unit cell element is $0.19\lambda_0$ at 2.45 GHz frequency. The developed FSS is tested using VNA for its transmission parameters where the test results are found as per desired. The developed FSS rejects the 2.45 GHz, 3.5 GHz, and 5.8 GHz frequency bands with a 10 dB rejection bandwidth of 0.46 GHz, 0.26 GHz and 1.68 GHz, respectively. These bands correspond to Wi-Fi, WiMax, and ISM/WiMax in general. The developed FSS is prototype of RF shielding structure which has to be utilized for the fabrication of an interference-free test chamber that isolates the Wi-Fi, WiMax, and ISM/WiMax interferences. By taking into consideration the application, FSS design has been selected very simple with single side printing which reduces the fabrication complexity required for production at large scale. The developed prototype has wide application scopes mainly in the area of defence sites, medical facilities (ICU), prison cells, worship places, etc. because of its simple design and easy production.

ACKNOWLEDGEMENT

REFERENCES

[1] Munk, B. A., *Frequency Selective Surfaces: Theory and Design*, John Wiley & Sons, 2005.

[2] Syed, I. S., Y. Ranga, L. Matekovits, K. P. Esselle, and S. G. Hay, "A single-layer frequency-selective surface for ultrawide-band electromagnetic shielding," *IEEE Transactions on Electromagnetic Compatibility*, Vol. 56, No. 6, 1404–1411, 2014.

[3] Fang, C. Y., J. S. Gao, and H. Liu, "A novel metamaterial filter with stable passband performance based on frequency selective surface," *AIP Advances*, Vol. 4, No. 7, 077114, 2014.

[4] Genovesi, S., F. Costa, and A. Monorchio, "Low-profile array with reduced radar cross section by using hybrid frequency selective surfaces," *IEEE Transactions on Antennas and Propagation*, Vol. 60, No. 5, 2327–2335, 2012.

[5] Costa, F. and A. Monorchio, "A frequency selective radome with wideband absorbing properties," *IEEE Transactions on Antennas and Propagation*, Vol. 60, No. 6, 2740–2747, 2012.

[6] Farooq, U., M. F. Shafique, and M. J. Mughal, "Polarization insensitive dual band frequency selective surface for RF shielding through glass windows," *IEEE Transactions on Electromagnetic Compatibility*, Vol. 62, No. 1, 93–100, 2020.

[7] Da Silva Segundo, F. C. G. and A. L. P. S. Campos, "Compact frequency selective surface with dual band response for WLAN applications," *Microwave and Optical Technology Letters*, Vol. 57, No. 2, 265–268, 2015.

[8] Yadav, S., C. P. Jain, and M. M. Sharma, "Polarization independent dual-bandpass frequency selective surface for Wimax applications," *International Journal of RF and Microwave Computer-Aided Engineering*, Vol. 28, No. 6, e21278, 2018.

[9] Bashiri, M., C. Ghobadi, J. Nourinia, and M. Majidzadeh, "WiMAX, WLAN, and X-band filtering mechanism: Simple-structured triple-band frequency selective surface," *IEEE Antennas and Wireless Propagation Letters*, Vol. 16, 3245–3248, 2017.

[10] Ghosh, S. and S. Lim, "A miniaturized bandpass frequency selective surface exploiting three-dimensional printing technique," *IEEE Antennas and Wireless Propagation Letters*, Vol. 18, No. 7, 1322–1326, 2019.

[11] Langley, R. J. and E. A. Parker, "Equivalent circuit model for arrays of square loops," *Electronics Letters*, Vol. 18, 294–296, 1982.

[12] Jha, K. R., G. Singh, and R. Jyoti, "A simple synthesis technique of single-square-loop frequency selective surface," *Progress In Electromagnetics Research B*, Vol. 45, 165–185, 2012.

[13] Sarabandi, K. and N. Behdad, "A frequency selective surface with miniaturized elements," *IEEE Transactions on Antennas and Propagation*, Vol. 55, No. 5, 1239–1245, 2007.

[14] Sievenpiper, D. F., *High-impedance Electromagnetic Surfaces*, University of California, Los Angeles, 1999.

[15] Jangi Golezani, J., M. Kartal, B. Doken, and S. Paker, "Triple-band frequency selective surface design effective over oblique incidence angles for GSM system," *IETE Journal of Research*, Vol. 68, No. 2, 1406–1410, 2022.

[16] Natarajan, R., M. Kanagasabai, S. Baisakhiya, R. Sivasamy, S. Palaniswamy, and J. K. Pakkathillam, "A compact frequency selective surface with stable response for WLAN applications," *IEEE Antennas and Wireless Propagation Letters*, Vol. 12, 718–720, 2013.

[17] Sivasamy, R., L. Murugasamy, M. Kanagasabai, E. F. Sundarsingh, and M. G. N. Alsath, "A low-profile paper substrate-based dual-band FSS for GSM shielding," *IEEE Transactions on Electromagnetic Compatibility*, Vol. 58, No. 2, 611–614, 2016.

[18] Unaldi, S., S. Cimen, G. Cakir, and U. E. Ayten, "A novel dual-band ultrathin FSS with closely settled frequency response," *IEEE Antennas and Wireless Propagation Letters*, Vol. 16, 1381–1384, 2016.